

## Contact Fatigue in Silicon Nitride

Seung Kun Lee\*<sup>†</sup> and Brian R. Lawn\*

Materials Science and Engineering Laboratory, National Institute of Standards and Technology, Gaithersburg, Maryland 20899

**A study of contact fatigue in silicon nitride is reported. The contacts are made using WC spheres, principally in cyclic but also in static loading, and mainly in air but also in nitrogen and water. Damage patterns are examined in three silicon nitride microstructures: (i) fine (*F*)—almost exclusively fully-developed cone cracks; (ii) medium (*M*)—well developed but smaller cone cracks, plus modest sub-surface quasi-plastic damage; (iii) coarse (*C*)—intense quasi-plastic damage, with little or no cone cracking. The study focuses on the influence of these competing damage types on inert strength as a function of number of contacts. In the *F* and *M* microstructures strength degradation is attributable primarily to chemically assisted slow growth of cone cracks in the presence of moisture during contact, although the *M* material shows signs of enhanced failure from quasi-plastic zones at large number of cycles. The *C* microstructure, although relatively tolerant of single-cycle damage, shows strongly accelerated strength losses from mechanical degradation within the quasi-plastic damage zones in cyclic loading conditions, especially in water. Implications concerning the design of silicon nitride microstructures for long-lifetime applications, specifically in concentrated loading, are considered.**

## I. Introduction

IT IS well known that increasing microstructural heterogeneity (e.g., by coarsening and elongating grains, and introducing weak boundaries) toughens ceramics in the long-crack region, primarily by enhancing bridging.<sup>1-5</sup> It also renders these same ceramics more susceptible to fatigue in cyclic loading, by degrading the bridging<sup>6,7</sup>—enhanced toughness and improved fatigue resistance tend to be mutually exclusive. This inverse relation between fatigue susceptibility and toughness extends even to strong ceramics like silicon nitride.<sup>8-10</sup>

Susceptibility of tough ceramics to fatigue is even more dramatic in Hertzian contacts, where the applied stresses are intense and localized.<sup>11-13</sup> In the present paper we investigate the influence of microstructure on Hertzian contact fatigue in silicon nitride, by conducting tests on three microstructures (“fine” (*F*), “medium” (*M*), and “coarse” (*C*)) from an earlier two-part study on contact damage in single-cycle loading.<sup>14,15</sup> Those earlier studies revealed a fundamental change in contact damage mode and ensuing failure origin in the three microstructures: from macroscopic cone cracks in the finest, most homogeneous *F* structure, to diffuse shear fault damage zones

in the coarsest, most heterogeneous *C* structure. The questions arise: How does the microstructure affect the fatigue and strength after repeated contacts, and what are the contact fatigue properties?

Accordingly, we present indentation-fatigue data on our selected silicon nitrides. Specifically, we investigate the inert strengths of contact-damaged specimens as a function of number of cycles at specified contact loads, predominantly under cyclic but also under static loading, in different environments—air, nitrogen, and water. We demonstrate that the tougher, more heterogeneous microstructures, while more damage tolerant in single-cycle loading, are prone to accelerated strength degradation in extreme loading conditions, i.e., high numbers of cycles (and loads) and moist environments. The issue of mechanical vs chemical fatigue is addressed, and conditions for strength degradation thresholds are summarized in “design maps.”

## II. Experimental Procedure

## (1) Materials Selection and Characterization

As indicated, the silicon nitride materials used here are from an earlier study:<sup>14</sup> (i) “fine” (*F*-Si<sub>3</sub>N<sub>4</sub>), a bimodal microstructure with ≈75 vol% equiaxed α grains of mean size ≈0.4 μm and ≈15 vol% elongated β grains of length 1.5 μm and diameter 0.4 μm; (ii) “medium” (*M*-Si<sub>3</sub>N<sub>4</sub>), a bimodal microstructure with ≈20 vol% equiaxed α grains of mean size ≈0.5 μm and ≈70 vol% elongated β grains of length 4.0 μm and diameter 0.5 μm; (iii) “coarse” (*C*-Si<sub>3</sub>N<sub>4</sub>), a microstructure with elongated β grains of mean length ≈9 μm and diameter 1.5 μm. Each material contains ≈10 vol% interboundary glassy phase.

The nature of single-cycle contact damage in these silicon nitrides, using tungsten carbide (WC) spheres of radius  $r = 1.98$  mm in air, has been previously reported.<sup>14</sup> Figure 1 reproduces top-surface and side-section views of typical damage patterns from that earlier work: (a) *F*-Si<sub>3</sub>N<sub>4</sub>, large cone cracks, no detectable quasi-plasticity; (b) *M*-Si<sub>3</sub>N<sub>4</sub>, smaller but still well-developed cone cracks, modest quasi-plasticity; (c) *C*-Si<sub>3</sub>N<sub>4</sub>, vestigial surface ring cracks, dominant quasi-plasticity. Figure 2 summarizes corresponding critical loads to initiate full cone cracks,  $P_C$ , and quasi-plastic yield zones,  $P_Y$ ;  $P_C$  increases in the sequence  $F \rightarrow M \rightarrow C$  (until, in *C*, no full cone is produced at all up to  $P = 4000$  N); conversely,  $P_Y$  decreases in the same sequence.

In the present work cyclic Hertzian indentations were made on the top surfaces of polished specimens 3 mm × 4 mm × 25 mm using the same WC spheres,  $r = 1.98$  mm, up to  $n = 10^7$  at frequency 10 Hz with havesinusoidal waveform (zero to maximum load), on a servo-hydraulic universal testing machine (Model 8502, Instron Corp., Canton, MA). These tests were run mainly in air (relative humidity ≈ 50%), but also in distilled water and dry nitrogen. Some comparative indentation tests were made at static contact loads to isolate any mechanical contribution to the damage accumulation. The WC spheres tended to deform during the extended contacts<sup>14</sup> and were rotated or replaced after each test.

Indented surfaces were gold coated and examined in Nomarski illumination. Some specimens were serial-polished from the top surface to reveal the depth of damage.

J. E. Ritter Jr.—contributing editor

Manuscript No. 190188. Received May 18, 1998; approved September 30, 1998. Supported by the U.S. Air Force Office of Scientific Research.

\*Member, American Ceramic Society.

†Now at Advanced Materials Technology, Technical Center, Caterpillar Inc., Moline, Illinois 61552.

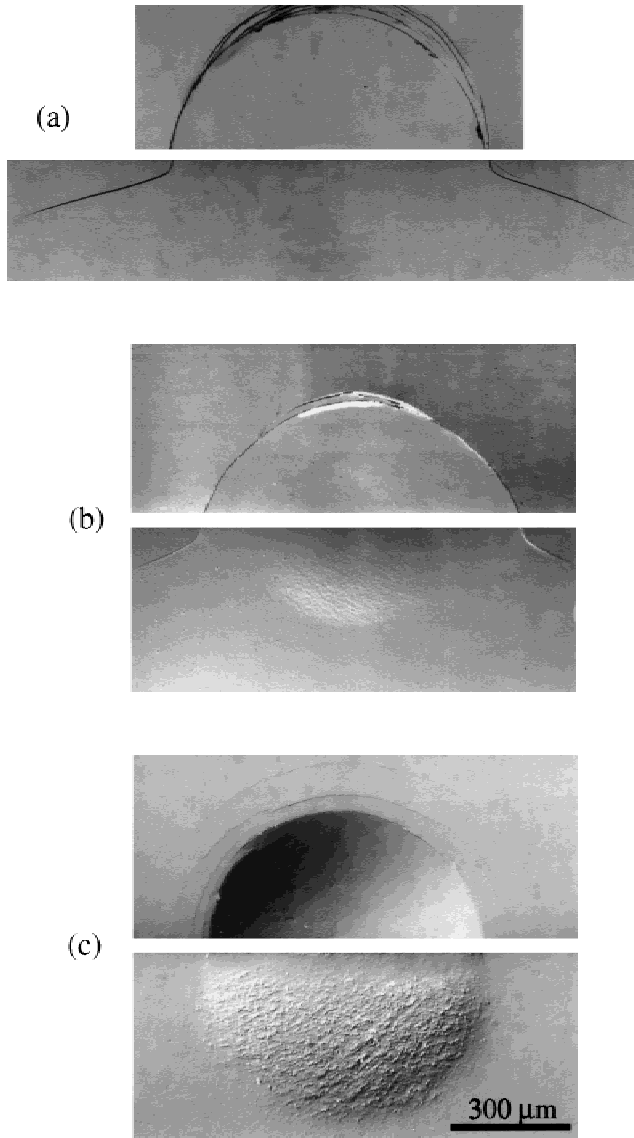


**Fig. 1.** Half-surface and side views of single-cycle Hertzian contact damage in (a)  $F\text{-Si}_3\text{N}_4$ , (b)  $M\text{-Si}_3\text{N}_4$ , (c)  $C\text{-Si}_3\text{N}_4$ , from WC sphere of radius  $r = 1.98$  mm at load  $P = 4000$  N, in air. Nomarski optical micrographs of bonded-interface specimens. Reproduced from Ref. 14.

## (2) Strength Tests

Strength tests were run on the  $3\text{ mm} \times 4\text{ mm} \times 25\text{ mm}$  polished bar specimens in four-point flexure, inner span 10 mm and outer span 20 mm, with the indentation sites centered on the tensile faces. Prior to indentation, the bar edges were chamfered and polished to minimize edge failures. All indentation sites were covered by a drop of silicone oil before testing and the bars broken in fast fracture ( $<10$  ms) to avoid the influence of moisture (“inert” strengths). Broken specimens were examined fractographically to locate the source of failure, either extraneous natural flaws or indentations—in the latter case distinction was made between failures from cone cracks and quasi-plastic zones.<sup>15,16</sup>

Previous control inert strength tests on unindented controls gave baseline “laboratory” strengths  $885 \pm 85$  MPa for  $F\text{-Si}_3\text{N}_4$ ,  $1084 \pm 62$  MPa for  $M\text{-Si}_3\text{N}_4$ , and  $792 \pm 32$  MPa for  $C\text{-Si}_3\text{N}_4$ , consistent with relative toughness levels and flaw sizes.<sup>14,15</sup> Note that the intermediate  $M$  material has the greatest strength of the three materials, owing to a favorable combination of enhanced  $\beta$  phase and moderate flaw size.<sup>14</sup>

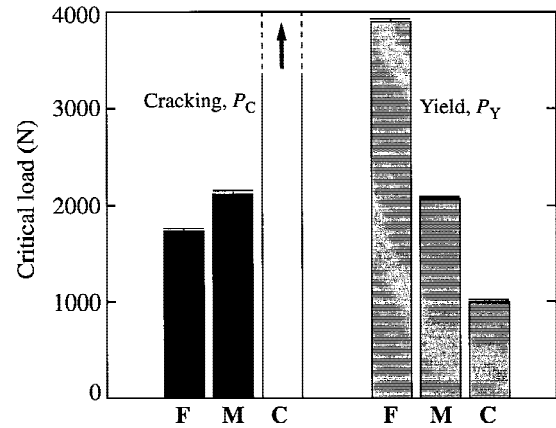


**Fig. 2.** Critical loads for onset of first full cone cracking,  $P_C$ , and subsurface yield,  $P_Y$ , in single-cycle loading, WC sphere  $r = 1.98$  mm, in air. Black bars indicate full cone cracks, open bars no cone cracks. Gray bars indicate yield. Data from Ref. 14.

## III. Results

Results from the indentation–strength tests on the three silicon nitride materials are presented in the following subsections as plots of strength  $\sigma_F$  as a function either of load  $P$  at fixed cycles  $n$ , or number of contact cycles  $n$  (or equivalent contact time) at fixed load  $P$ . In all such plots data points are means and

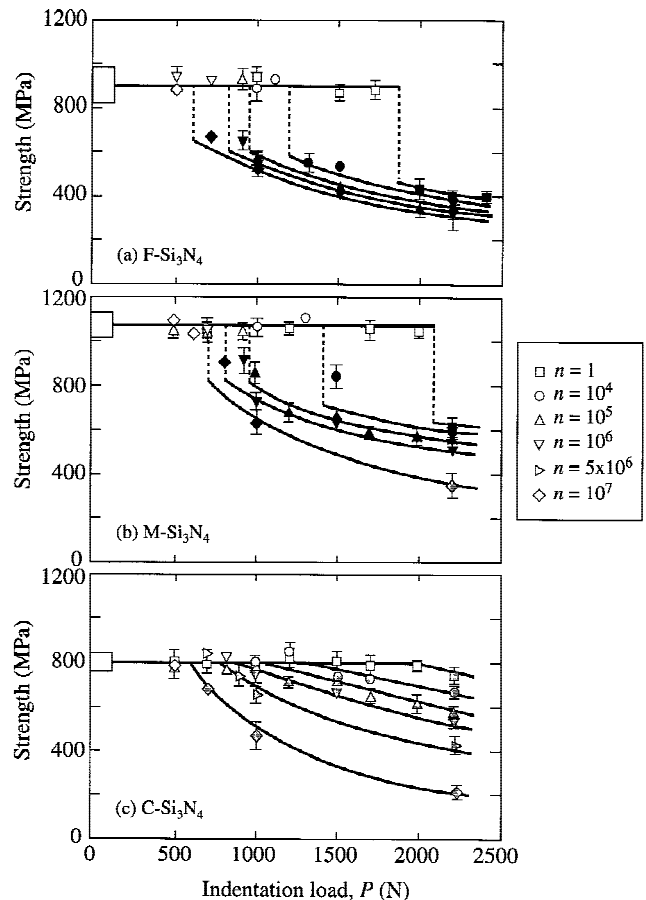


**Fig. 3.** Strength as a function of contact load for (a)  $F\text{-Si}_3\text{N}_4$ , (b)  $M\text{-Si}_3\text{N}_4$ , (c)  $C\text{-Si}_3\text{N}_4$ , demonstrating role of microstructure. Indentation with WC spheres,  $r = 1.98$  mm, in air, at specified  $n$  cycles. Black symbols indicate failure from cone cracks, gray symbols from quasi-plastic zones, open symbols from natural flaws. Boxes at left axis indicate “laboratory” strengths.

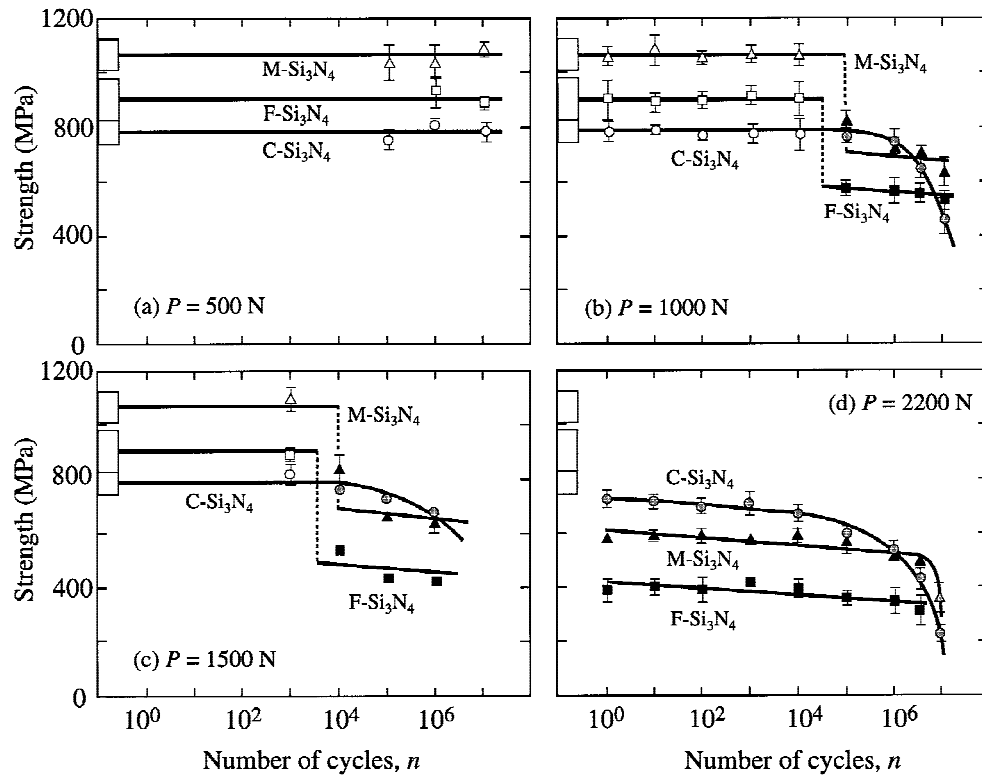


**Fig. 4.** Strength as a function of number of contact cycles for  $F-Si_3N_4$ ,  $M-Si_3N_4$ ,  $C-Si_3N_4$ , demonstrating role of microstructure. Indentation with WC spheres,  $r = 1.98$  mm, in air, at loads  $P =$  (a) 500, (b) 1000, (c) 1500, and (d) 2200 N. Black symbols indicate failure from cone cracks, gray symbols from quasi-plastic zones, and open symbols from natural flaws. Boxes at left axis indicate "laboratory" strengths.

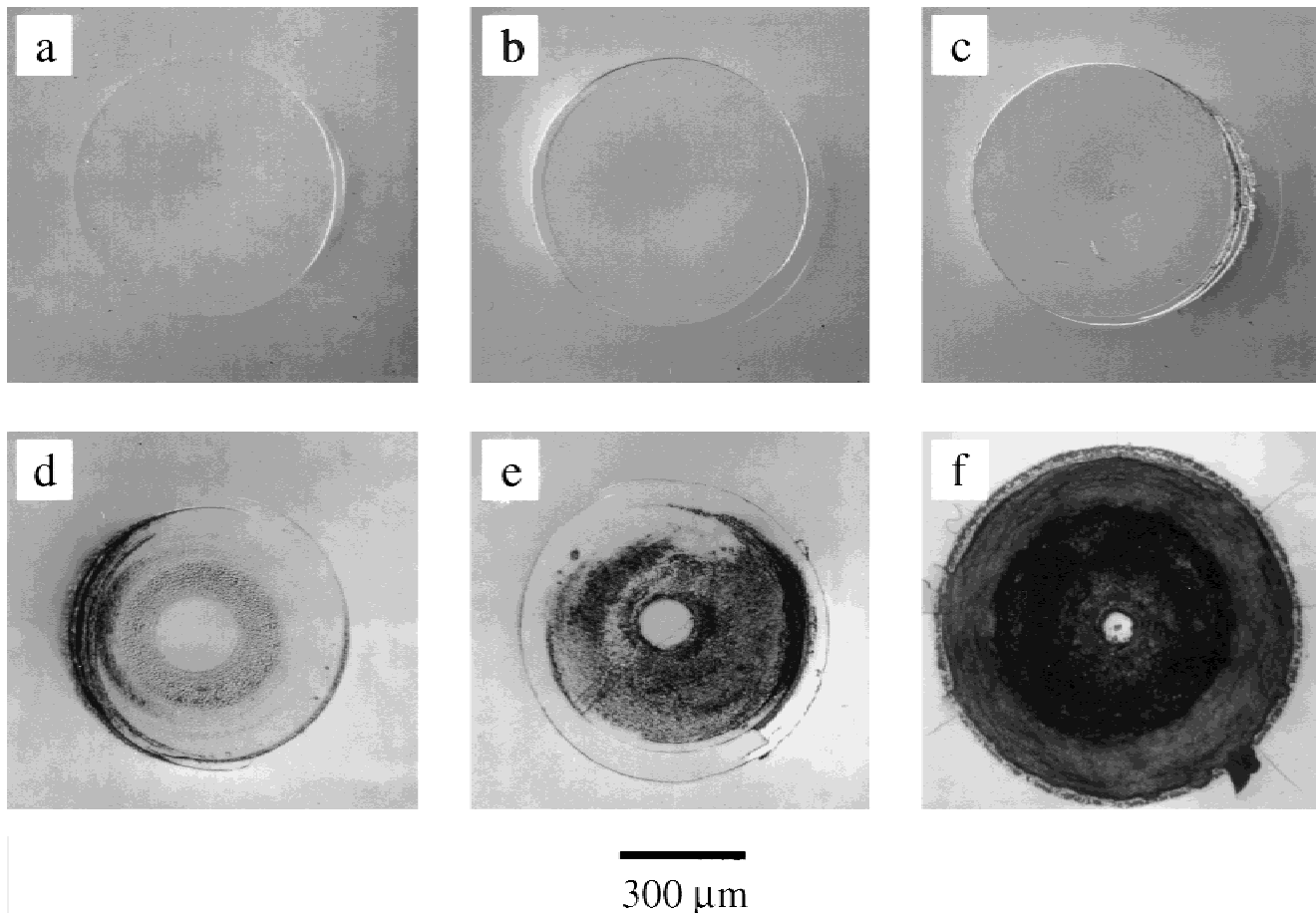


**Fig. 5.** Surface damage in  $M-Si_3N_4$  after indentation with WC spheres,  $r = 1.98$  mm,  $P = 2200$  N, in air:  $n =$  (a) 1, (b)  $10^3$ , (c)  $10^4$ , (d)  $10^5$ , (e)  $10^6$ , and (f)  $10^7$  cycles. Ring cracks are surface traces of fully developed cones. Limited quasi-plasticity within the contact area becomes detectable as  $n$  increases, augmented at high  $n$  by surface fretting damage.

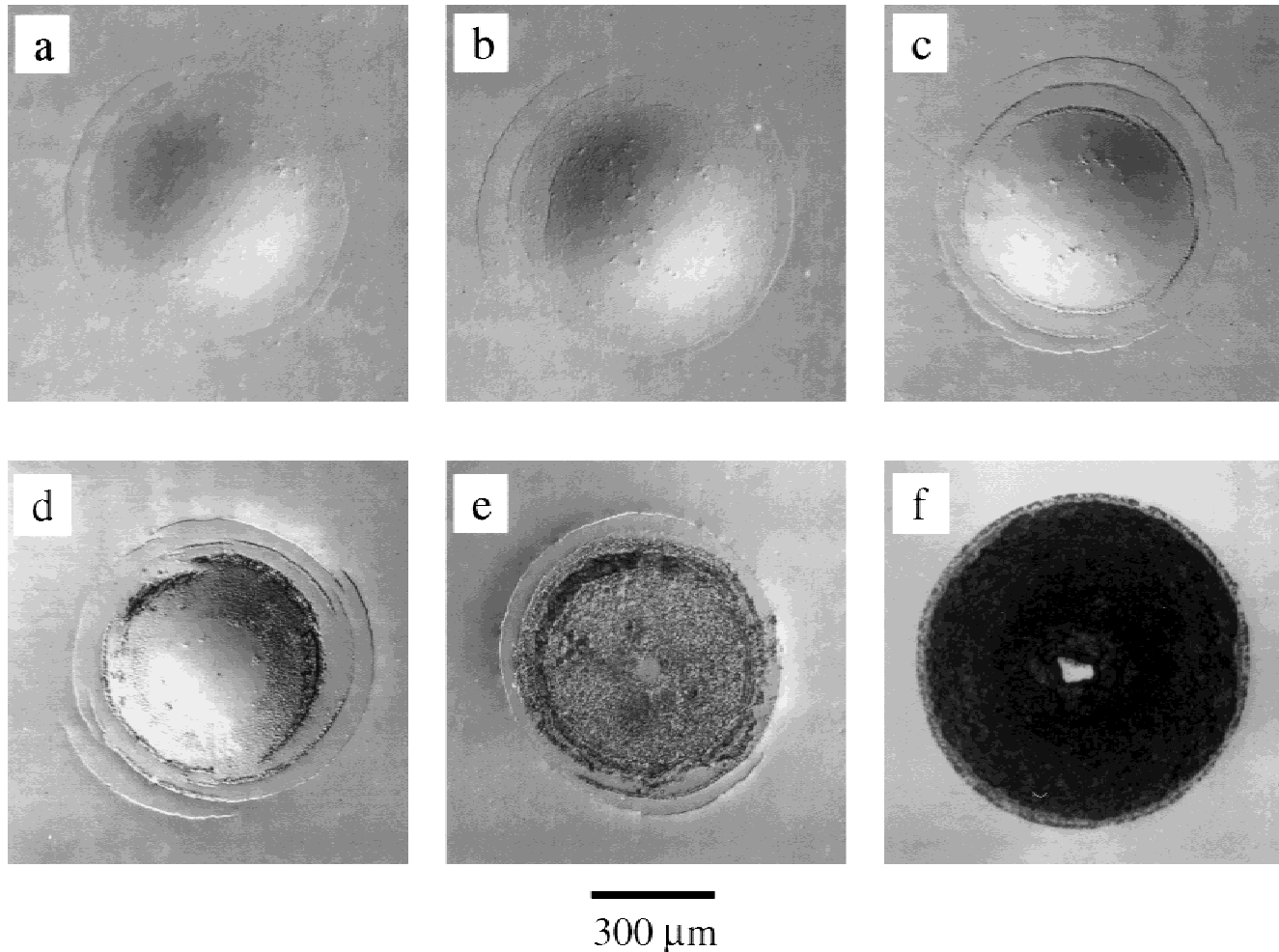


**Fig. 6.** Surface damage in  $C\text{-Si}_3\text{N}_4$  after indentation with WC spheres,  $r = 1.98$  mm,  $P = 2200$  N, in air:  $n =$  (a) 1, (b)  $10^3$ , (c)  $10^4$ , (d)  $10^5$ , (e)  $10^6$ , and (f)  $10^7$  cycles. Ring cracks are only “skin deep” in this material. Quasi-plasticity within the contact area is apparent even at low  $n$ , again with accompanying surface fretting damage at high  $n$ .

standard deviations of inert strengths for an average of four specimens—black symbols represent failures from cone cracks, gray symbols from quasi-plastic zones, and open symbols from natural flaws. Boxes at left represent strengths of unindented specimens. Solid curves are empirical fits through the data.

#### (1) Role of Microstructure

In this section we consider the role of microstructure on the contact fatigue of silicon nitride, for contact tests in air. Figure 3 plots inert strength  $\sigma_F$  as a function of load  $P$  for  $F\text{-Si}_3\text{N}_4$ ,  $M\text{-Si}_3\text{N}_4$ , and  $C\text{-Si}_3\text{N}_4$ , at specified numbers of cycles over the range  $n = 1$  to  $10^7$ :

(a) Figure 3(a),  $F\text{-Si}_3\text{N}_4$ : Strengths initially remain steady with increasing load at the laboratory (unindented) value, corresponding to failure from natural flaws. At some threshold load the strength drops off abruptly, as cone cracks initiate. Thereafter, the strengths decline only slightly with load, as the now-stable cone cracks extend deeper into the subsurface.<sup>15</sup> The threshold loads diminish rapidly with increasing  $n$  (cf.  $P_C \approx 1800$  N at  $n = 1$ , Fig. 2), consistent with some kinetic effect in the initial cone crack evolution during contact.<sup>17,18</sup> In the post-threshold region, the strengths decline modestly with increasing  $n$ , suggesting slow extensions of the fully developed cone cracks during cycling.

(b) Figure 3(b),  $M\text{-Si}_3\text{N}_4$ : The trends are similar to those for the  $F$  material, indicating a common cone-crack failure mode, again with ever-diminishing threshold loads (cf.  $P_C \approx$

2150 N, Fig. 2). Relative to  $F\text{-Si}_3\text{N}_4$ , the data appear to be a little more sensitive to  $n$  in this material: the strength levels are somewhat higher, except at the highest values of  $P$  (2200 N) and  $n$  ( $10^7$ ), where failure originates from quasi-plastic zones (cf.  $P_Y \approx 2050$  N, Fig. 2). Thus the quasi-plastic damage mode, initially subservient to the cone cracking in this material, ultimately leads to accelerated breakdown.

(c) Figure 3(c),  $C\text{-Si}_3\text{N}_4$ : Strengths are steady up to a threshold degradation load, beyond which the strengths decline without discontinuity.<sup>16</sup> In this latter region failures occur exclusively from quasi-plastic zones. The loads at first degradation diminish markedly with increasing  $n$  (cf.  $P_Y \approx 1000$  N, Fig. 2), as do the ensuing strength levels, indicating accelerated damage accumulation in the quasi-plasticity mode.

Intercomparisons between the three silicon nitride microstructures are brought out more clearly in Fig. 4, which plots  $\sigma_F(n)$  strength data for  $F\text{-Si}_3\text{N}_4$ ,  $M\text{-Si}_3\text{N}_4$ , and  $C\text{-Si}_3\text{N}_4$  after indentation at four specified loads  $P$  in air. The selected loads embrace a broad range relative to the critical loads for cracking ( $P_C$ ) and yield ( $P_Y$ ) in single-cycle loading (Fig. 2):

(a) Figure 4(a),  $P = 500$  N ( $\ll P_C$ ,  $\ll P_Y$  in all materials): Strengths remain undiminished from their laboratory (unindented) values over the entire cyclic range up to  $n = 10^7$ .

(b) Figure 4(b),  $P = 1000$  N ( $< P_C$  in all three materials;  $< P_Y$  except for  $C\text{-Si}_3\text{N}_4$ , where  $\approx P_Y$ ): Up to a threshold number of cycles the strengths remain undiminished, and failures occur from natural flaws. At higher  $n$  the strengths degrade, and failures initiate from cone cracks or quasi-plastic zones. In

$F\text{-Si}_3\text{N}_4$  and  $M\text{-Si}_3\text{N}_4$ , at a threshold number of cycles somewhere in the range  $n = 10^4\text{--}10^5$ , the strengths undergo abrupt strength drops of 30–40%. By contrast, initial degradation in the  $C\text{-Si}_3\text{N}_4$  at  $n \approx 10^5$  is gradual without apparent discontinuity. Strength degradation progresses thereafter in all materials up to  $n = 10^7$ : in the  $F$  and  $M$  materials this progressive degradation is relatively slight, suggesting minor continued cone crack extension; in the  $C$  material, however, the degradation accelerates rapidly until, ultimately, its strength drops below those of its  $F$  and  $M$  counterparts. Note that the  $M$  material has the highest initial and final strengths.

(c) Figure 4(c),  $P = 1500$  N ( $<P_C$  in all three materials;  $<P_Y$  except for  $C\text{-Si}_3\text{N}_4$ ): The failure origins are unchanged in the degradation region—cone cracks in  $F\text{-Si}_3\text{N}_4$  and  $M\text{-Si}_3\text{N}_4$ , quasi-plastic zones in  $C\text{-Si}_3\text{N}_4$ . The strengths now hold their value only up to  $n \approx 10^3\text{--}10^4$  for  $F\text{-Si}_3\text{N}_4$  and  $M\text{-Si}_3\text{N}_4$ ,  $n \approx 10^4$  for  $C\text{-Si}_3\text{N}_4$ . At higher  $n$  the data trends are similar to those at  $P = 1000$  N, except that the degraded strengths are a little lower. Again, the degradation in the  $C$  material accelerates at high  $n$ , relative to the  $F$  and  $M$  materials.

(d) Figure 4(d),  $P = 2200$  N ( $>P_C$  in  $F\text{-Si}_3\text{N}_4$  and  $M\text{-Si}_3\text{N}_4$ , but  $<<P_C$  for  $C\text{-Si}_3\text{N}_4$ ;  $<<P_Y$  for  $F\text{-Si}_3\text{N}_4$ ,  $\approx P_Y$  for  $M\text{-Si}_3\text{N}_4$ , and  $>>P_Y$  for  $C\text{-Si}_3\text{N}_4$ ): A significant amount of damage is introduced at  $n = 1$  in all three materials, so that strength drops occur after the first cycle. The decrements are substantial in  $F\text{-Si}_3\text{N}_4$  and  $M\text{-Si}_3\text{N}_4$ , consistent with cone-crack failure origins, but slight in  $C\text{-Si}_3\text{N}_4$ , consistent with quasi-plastic zone origins. The ensuing strengths decline only slightly from the initial degraded values up to  $n \approx 10^5$ . Beyond this number of cycles, however, the decline is more rapid, especially in the  $C$  material. Ultimately, at  $n = 10^7$ , breaks occur from intensely developed quasi-plastic zones in both  $C$  and  $M$  materials.

The damage evolution leading to the accelerated cyclic degradation in the  $M\text{-Si}_3\text{N}_4$  and  $C\text{-Si}_3\text{N}_4$  materials in Fig. 4(d) (i.e., for  $P = 2200$  N in air) is shown in the surface micrographs in Figs. 5 and 6. In  $M\text{-Si}_3\text{N}_4$  (Fig. 5) surface ring cracks are apparent at  $n = 1$ , and become even more clearly defined as  $n$  increases. Minor residual surface depressions appear at  $n \approx 10^3\text{--}10^4$ , accompanied by surface “fretting” damage at higher  $n$ .<sup>19–21</sup> Ultimately, at  $n = 10^7$ , the surface damage is severe, with material removal within the contact area and incipient radial cracking at the periphery. Serial polishing  $\approx 50$   $\mu\text{m}$  from the top surface leaves the ring cracks intact at all  $n$  (confirming completely formed cones—cf. Fig. 1(b)) and removes all of the fretting damage up to  $n = 10^6$ , consistent with an essentially brittle response. At  $n = 10^7$ , however, the fretting damage persists after polishing, indicating an enhanced subsurface yield zone with microcrack coalescence. It is this enhanced quasi-plastic zone that provides the sources of failure in  $M\text{-Si}_3\text{N}_4$  at extreme loading conditions in Figs. 3(b) and 4(d).<sup>15</sup> In  $C\text{-Si}_3\text{N}_4$  (Fig. 6) surface ring cracks are again evident, although considerably less distinct than in  $M\text{-Si}_3\text{N}_4$ . On the other hand, residual surface depressions are much more pronounced at all  $n$  values. Surface polishing confirms that the ring cracks are only “skin deep,” and that the quasi-plastic zones extend well into the subsurface, at all  $n$  (cf. Fig. 1(c)). Fretting damage is again especially severe at  $n = 10^7$ , further enhancing the quasi-plastic damage with resultant accelerated damage coalescence and contact fatigue.

## (2) Role of Environment

Figure 7 plots inert strength  $\sigma_F(P)$  data for tests on  $F\text{-Si}_3\text{N}_4$ ,  $M\text{-Si}_3\text{N}_4$ , and  $C\text{-Si}_3\text{N}_4$  at  $n = 10^5$  cycles in laboratory air, dry nitrogen, and water. Above load thresholds failures again originate from cone cracks in  $F$  (Fig. 7(a)) and  $M$  (Fig. 7(b)) materials, and from quasi-plastic zones in  $C$  (Fig. 7(c)). These data confirm pronounced chemical effects in all three grades of material. The threshold loads for the onset of strength degradation are especially sensitive to environment, diminishing strongly with increasing moisture content. At larger  $P$  the

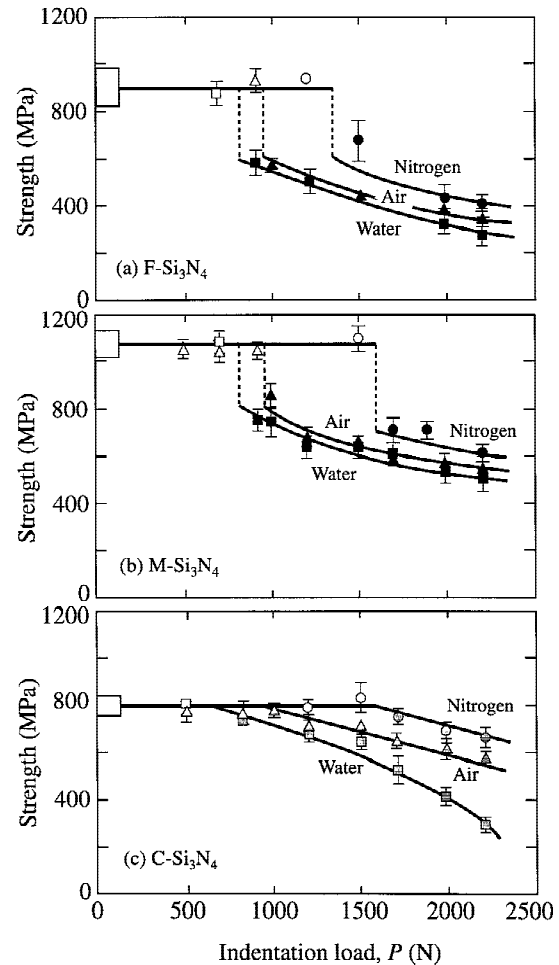


**Fig. 7.** Strength as a function of contact load for (a)  $F\text{-Si}_3\text{N}_4$ , (b)  $M\text{-Si}_3\text{N}_4$ , (c)  $C\text{-Si}_3\text{N}_4$ , demonstrating effect of environment. Indentation with WC spheres,  $r = 1.98$  mm,  $n = 10^5$ , in laboratory air, dry nitrogen, and water. Black symbols indicate failure from cone cracks, gray symbols from quasi-plastic zones, and open symbols from natural flaws. Boxes at left axis indicate “laboratory” strengths.

strengths show different sensitivities to moisture content: relatively mild in the  $F$  and  $M$  materials, more severe in  $C$ . Once more,  $C\text{-Si}_3\text{N}_4$  shows the most excessive degradation in extreme conditions.

Figure 8 compares micrographs of contact surface damage in the three silicon nitrides in air and water environments, at  $P = 2200$  N. The presence of water clearly enhances the surface damage, especially in  $C\text{-Si}_3\text{N}_4$ , where material removal and incipient radial cracking are again apparent, but also to some extent in  $F\text{-Si}_3\text{N}_4$ , where a collar of material has become detached outside the cone crack trace.<sup>13</sup> The enhanced surface damage in  $C\text{-Si}_3\text{N}_4$  correlates with the accelerated strength falloff in the water environment (Fig. 7(c)). Interestingly, the enhanced surface damage in  $F\text{-Si}_3\text{N}_4$  has relatively little effect on the strength (Fig. 7(a)), consistent with failure from deeper cone cracks in the finer, more brittle microstructures.<sup>13</sup>

## (3) Cyclic vs Static Fatigue

Figure 9 compares  $\sigma_F(n)$  inert strength data for cyclic and static contacts in  $F\text{-Si}_3\text{N}_4$ ,  $M\text{-Si}_3\text{N}_4$ , and  $C\text{-Si}_3\text{N}_4$ , at  $P = 2200$  N in air. The results are plotted as a function of contact time (upper axis) as well as number of cycles (lower axis), to facilitate direct intercomparisons. In the  $F$  and  $M$  materials the static data sets are barely distinguishable from the cyclic data sets over most of the data range (i.e., except perhaps at  $n = 10^7$  in  $M\text{-Si}_3\text{N}_4$ ). In the  $C$  material, on the other hand, the cyclic

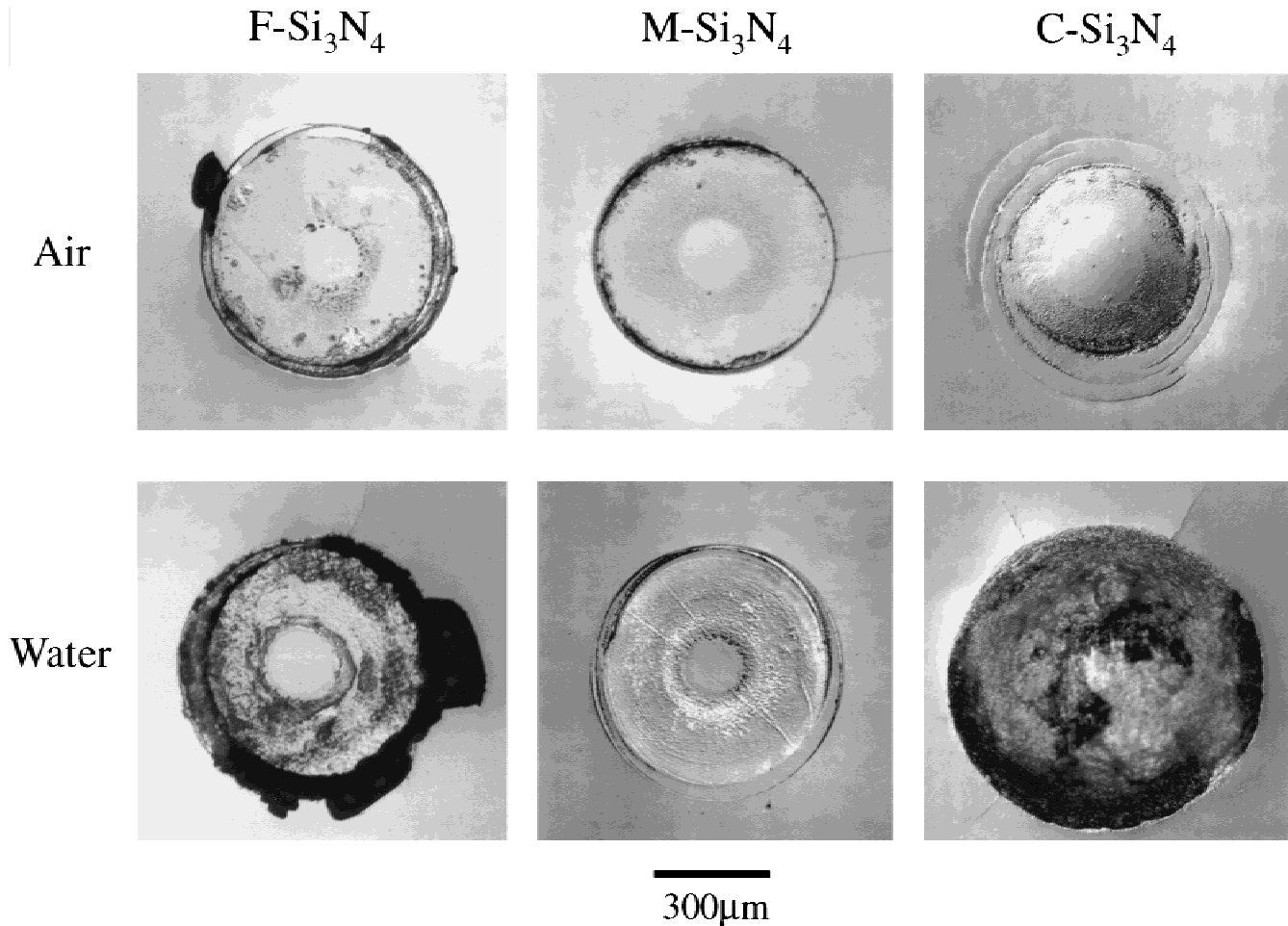


**Fig. 8.** Surface damage in  $F\text{-Si}_3\text{N}_4$ ,  $M\text{-Si}_3\text{N}_4$ , and  $C\text{-Si}_3\text{N}_4$  after indentation with WC spheres,  $r = 1.98$  mm,  $P = 2200$  N,  $n = 10^5$ , in air and water. Water clearly enhances the damage, especially in the  $C$  material.

data set falls significantly lower than the static data set, the more so at high  $n$ .

#### IV. Discussion

We have investigated the effect of cyclic contact on strength in  $F\text{-Si}_3\text{N}_4$  (fine),  $M\text{-Si}_3\text{N}_4$  (medium), and  $C\text{-Si}_3\text{N}_4$  (coarse) microstructures. The  $F$  and  $M$  materials show typically brittle responses (Figs. 3 and 4); beyond some threshold number of cycles  $n$ , failure originates from subsurface cone cracks instead of from natural microstructural flaws, with consequent abrupt dropoff in strength. Continued falloff in strength with higher  $n$  is relatively modest, confirming that the fully developed cone cracks are very stable.<sup>13,22,23</sup> However, in the  $M$  material at extreme loading conditions  $n = 10^7$ ,  $P = 2200$  N (Figs. 3(b) and 4(d)) the failure origin switches from cone crack to quasi-plastic zone, signaling the onset of a brittle-to-plastic transition.<sup>24</sup> In the  $C$  material failure occurs exclusively from quasi-plasticity zones,<sup>14</sup> initially with gradual but thereafter with rapid declines in strength. The transitional  $M$  microstructure has the highest strengths at the initial and final (although not intermediate) points of the cyclic range, and thereby represents a compromise between extremes of excessive brittleness and quasi-plasticity in bearing materials.<sup>14,15</sup>

The issue of damage thresholds is of particular interest in the context of design. We have alluded to the existence of critical loads for the onset of first visually detectable damage, either cracking or yield (Fig. 2). From the standpoint of lifetime the engineer is more likely to be concerned with the conditions that lead to first detectable *strength* degradation, i.e., where failures

first occur from the contact sites—either a threshold  $P$  at given  $n$  (Fig. 3) or a threshold  $n$  at given  $P$  (Fig. 4). Such threshold conditions are plotted for our three silicon nitrides on an  $(n,P)$  “design map” in Fig. 10, with failures from cone cracks and quasi-plastic zones appropriately distinguished. (The error bars in these plots reflect uncertainty bounds in the determinations from Figs. 3 and 4). The domain at lower left in Fig. 10 then indicates the zone of “safe” operation, where laboratory strengths are preserved. This domain, here specifically relating to tests with WC spheres  $r = 1.98$  mm in air, will shift with changes in such operational factors as sphere radius<sup>15</sup> and environment (Fig. 7). At first sight the plots in Fig. 10 appear not to be too different for the three materials, implying an insensitivity to microstructure. However, we emphasize that this figure represents only  $(n,P)$  loci of *first detectable* strength losses, and says nothing about actual *magnitudes* of these strength losses once degradation does set in: as noted in Figs. 3 and 4, the  $F$  and  $M$  materials suffer much higher strength decrements than in the  $C$  material at threshold; although, ultimately, the  $C$  material loses more strength at very high loads and numbers of cycles.

The presence of water during the contact process accelerates strength degradation in all three materials (Fig. 7), even in static loading (Fig. 9), confirming the existence of a chemical effect in the fatigue. Both the threshold conditions for initiating the damage and the ensuing strength losses are adversely affected. In the more brittle  $F\text{-Si}_3\text{N}_4$  and  $M\text{-Si}_3\text{N}_4$  materials the behavior is entirely consistent with conventional slow crack growth extension of the cone cracks,<sup>13</sup> except for  $M\text{-Si}_3\text{N}_4$  at  $n = 10^7$ . The fact that the strength levels for cyclic and static

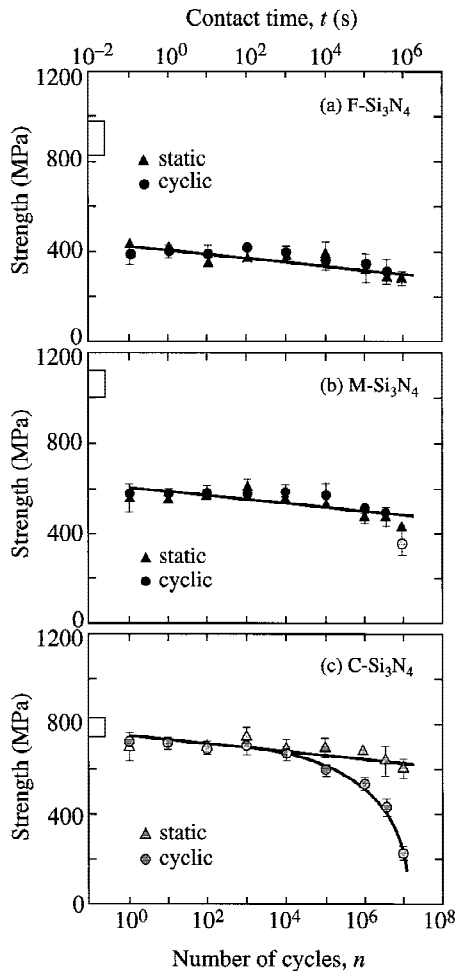


**Fig. 9.** Strength as a function of contact time for (a)  $F\text{-Si}_3\text{N}_4$ , (b)  $M\text{-Si}_3\text{N}_4$ , (c)  $C\text{-Si}_3\text{N}_4$ , comparing damage accumulation at static and cyclic contacts. Indentation with WC spheres,  $r = 1.98$  mm,  $P = 2200$  N, in air. Black symbols indicate failure from cone cracks, gray symbols from quasi-plastic zones. Boxes at left axis indicate "laboratory" strengths.

loading in Figs. 9(a) and (b) are virtually indistinguishable in these two grades of material indicates a relatively low sensitivity to kinetics in silicon nitride, i.e., a large crack velocity exponent.<sup>9</sup> In the  $C\text{-Si}_3\text{N}_4$  the strengths are substantially lower for cyclic than for static loading at large  $n$  in Fig. 9, indicating a dominant (but not exclusive) mechanical component in the quasi-plasticity mode.<sup>9,13,25</sup> The presence of a mechanical component in this form of  $\text{Si}_3\text{N}_4$  is consistent with hysteresis observed in load–displacement cycles in tougher, more heterogeneous ceramics, indicative of a degenerative internal friction process.<sup>12</sup>

A detailed understanding of the fatigue processes from accumulated quasi-plastic damage in tough silicon nitride microstructures under fatigue conditions is not yet available at the micromechanical level. Simplistic models of shear fault responses in single-cycle loading<sup>26</sup> and of the associated degrading effects on strength from extension of "wing" cracks at the fault ends<sup>16</sup> are emerging. Mechanical fatigue is hypothesized to arise from cyclic attrition of internal frictional resistance at shear fault interfaces,<sup>25,27</sup> leading to progressive crack extension and corresponding strength loss. Under extreme loading conditions, i.e., high numbers of cycles and/or loads, these shear faults and microcracks are subject to coalescence, with attendant generation of radial cracks (Fig. 8).<sup>16</sup> Once coalescence sets in, strength falls off dramatically,<sup>13,16</sup> and grains are on the verge of wholesale detachment from the contact zone.<sup>13</sup>

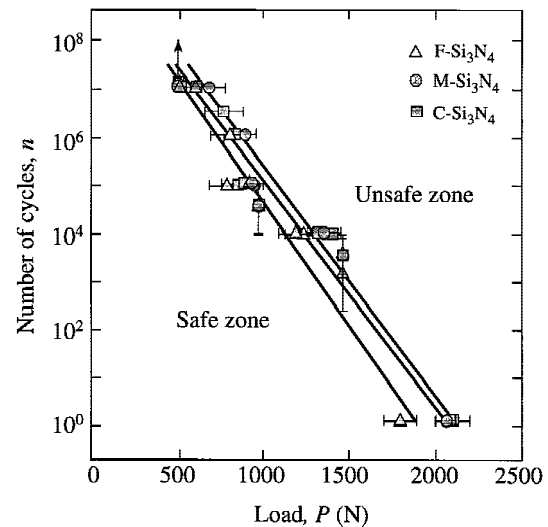


**Fig. 10.** Design map, number of cycles vs contact load for the onset of strength degradation in  $F\text{-Si}_3\text{N}_4$ ,  $M\text{-Si}_3\text{N}_4$ , and  $C\text{-Si}_3\text{N}_4$ , for indentations with WC spheres,  $r = 1.98$  mm, in air. Error bars indicate uncertainly bounds in threshold values of  $P$  at fixed  $n$  (Fig. 3) or  $n$  at fixed  $P$  (Fig. 4). Unsafe zone indicates domain in which natural strengths are compromised by damage accumulation.

The presence of water may diminish the frictional resistance at the shear faults still further, especially near the specimen surfaces where direct access is possible along coalescent crack pathways, as well as enhance extension of wing cracks.

The present results suggest that some compromise may be necessary in designing silicon nitrides or other ceramics for applications in repeat concentrated loads (e.g., bearings), especially in hostile chemical environments. Very fine silicon nitride microstructures ( $F\text{-Si}_3\text{N}_4$ ) are brittle and susceptible to abrupt strength losses above a threshold load. Very coarse microstructures ( $C\text{-Si}_3\text{N}_4$ ) are tough and show relatively small strength losses in first contact.<sup>14</sup> However, this apparently high damage tolerance in the coarse structures is somewhat deceptive: seemingly innocuous incipient damage from a single contact can accumulate steadily and inexorably as cycling continues, leading ultimately to excessive losses in strength (as well as in wear resistance). The optimization of silicon nitride microstructures for such applications clearly rests with a better understanding of the quasi-plastic damage accumulation processes.

Development of analytical fracture mechanics models for describing the strength degradation characteristics in brittle and quasi-plastic silicon nitride and other ceramics is under way.

**Acknowledgments:** We are grateful to D. K. Kim, K. S. Lee, N. P. Padture, and I. M. Peterson for useful discussions over the course of this work.

## References

- R. Knehan and R. Steinbrech, "Effect of Grain Size on the Resistance Curves of  $\text{Al}_2\text{O}_3$ "; pp. 613–19 in *Science of Ceramics*, Vol. 12. Edited by P. Vincenzini. Ceramurgica, Imola, Italy, 1983.
- P. L. Swanson, C. J. Fairbanks, B. R. Lawn, Y.-W. Mai, and B. J. Hockey, "Crack-Interface Grain Bridging as a Fracture Resistance Mechanism in Ceramics: I, Experimental Study on Alumina," *J. Am. Ceram. Soc.*, **70** [4] 279–89 (1987).
- S. J. Bennison and B. R. Lawn, "Role of Interfacial Grain-Bridging Sliding Friction in the Crack-Resistance and Strength Properties of Nontransforming Ceramics," *Acta Metall.*, **37** [10] 2659–71 (1989).
- S. J. Bennison and B. R. Lawn, "Flaw Tolerance in Ceramics with Rising Crack-Resistance Characteristics," *J. Mater. Sci.*, **24**, 3169–75 (1989).
- S. J. Bennison, N. P. Padture, J. L. Runyan, and B. R. Lawn, "Flaw-Insensitive Ceramics," *Philos. Mag. Lett.*, **64** [4] 191–95 (1991).
- S. Lathabai, Y.-W. Mai, and B. R. Lawn, "Cyclic Fatigue Behavior of an Alumina Ceramic with Crack-Resistance Curves," *J. Am. Ceram. Soc.*, **72** [9] 1760–63 (1989).

- <sup>7</sup>S. Lathabai, J. Rödel, and B. R. Lawn, "Cyclic Fatigue from Frictional Degradation at Bridging Grains in Alumina," *J. Am. Ceram. Soc.*, **74** [6] 1340–48 (1991).
- <sup>8</sup>R. H. Dauskardt, "A Frictional Wear Mechanism for Fatigue-Crack Growth in Grain Bridging Ceramics," *Acta Metall. Mater.*, **41** [9] 2765–81 (1993).
- <sup>9</sup>D. S. Jacobs and I-W. Chen, "Mechanical and Environmental Factors in the Cyclic and Static Fatigue of Silicon Nitride," *J. Am. Ceram. Soc.*, **77** [5] 1153–61 (1994).
- <sup>10</sup>C. J. Gilbert, R. H. Dauskardt, and R. O. Ritchie, "Behavior of Cyclic Fatigue Cracks in Monolithic Silicon Nitride," *J. Am. Ceram. Soc.*, **78** [9] 2291–300 (1995).
- <sup>11</sup>F. Guiberteau, N. P. Padture, H. Cai, and B. R. Lawn, "Indentation Fatigue: A Simple Cyclic Hertzian Test for Measuring Damage Accumulation in Polycrystalline Ceramics," *Philos. Mag. A*, **68** [5] 1003–16 (1993).
- <sup>12</sup>H. Cai, M. A. S. Kalceff, B. M. Hooks, B. R. Lawn, and K. Chyung, "Cyclic Fatigue of a Mica-Containing Glass-Ceramic at Hertzian Contacts," *J. Mater. Res.*, **9** [10] 2654–61 (1994).
- <sup>13</sup>N. P. Padture and B. R. Lawn, "Contact Fatigue of a Silicon Carbide with a Heterogeneous Grain Structure," *J. Am. Ceram. Soc.*, **78** [6] 1431–38 (1995).
- <sup>14</sup>S. K. Lee, S. Wuttiphon, and B. R. Lawn, "Role of Microstructure in Hertzian Contact Damage in Silicon Nitride: I, Mechanical Characterization," *J. Am. Ceram. Soc.*, **80** [9] 2367–81 (1997).
- <sup>15</sup>S. K. Lee and B. R. Lawn, "Role of Microstructure in Hertzian Contact Damage in Silicon Nitride: II, Strength Degradation," *J. Am. Ceram. Soc.*, **81** [4] 997–1003 (1998).
- <sup>16</sup>B. R. Lawn, S. K. Lee, I. M. Peterson, and S. Wuttiphon, "A Model of Strength Degradation From Hertzian Contact Damage in Tough Ceramics," *J. Am. Ceram. Soc.*, **81** [6] 1509–20 (1998).
- <sup>17</sup>F. B. Langitan and B. R. Lawn, "Effect of a Reactive Environment on the Hertzian Strength of Brittle Solids," *J. Appl. Phys.*, **41** [8] 3357–65 (1970).
- <sup>18</sup>A. G. Mikosza and B. R. Lawn, "Section-and-Etch Study of Hertzian Fracture Mechanics," *J. Appl. Phys.*, **42** [13] 5540–45 (1971).
- <sup>19</sup>K. L. Johnson, *Contact Mechanics*; Ch. 7. Cambridge University Press, London, U.K., 1985.
- <sup>20</sup>H. Makino, N. Kamiya, and S. Wada, "Grain Size Effects of Si<sub>3</sub>N<sub>4</sub> on Damage Morphology Induced by Localized Contact Stress"; pp. 229–34 in *Proceedings of the 1st International Symposium on the Science of Engineering Ceramics*. Edited by S. Kimura and K. Niihara. Koda, Aichi-Prefecture, Japan, 1991.
- <sup>21</sup>P. J. Kennedy, A. A. Conte, E. P. Whitemont, L. K. Ives, and M. B. Peterson, "Surface Damage and Mechanics of Fretting Wear in Ceramics"; pp. 79–98 in *Friction and Wear of Ceramics*. Edited by S. Jahanmir. Marcel Dekker, New York, 1994.
- <sup>22</sup>F. C. Roesler, "Brittle Fractures Near Equilibrium," *Proc. Phys. Soc. London*, **B69**, 981–92 (1956).
- <sup>23</sup>B. R. Lawn and T. R. Wilshaw, "Indentation Fracture: Principles and Applications," *J. Mater. Sci.*, **10** [6] 1049–81 (1975).
- <sup>24</sup>B. R. Lawn, N. P. Padture, H. Cai, and F. Guiberteau, "Making Ceramics 'Ductile'," *Science*, **263**, 1114–16 (1994).
- <sup>25</sup>N. P. Padture and B. R. Lawn, "Fatigue in Ceramics with Interconnecting Weak Interfaces: A Study Using Cyclic Hertzian Contacts," *Acta Metall.*, **43** [4] 1609–17 (1995).
- <sup>26</sup>B. R. Lawn and D. B. Marshall, "Nonlinear Stress–Strain Curves for Solids Containing Closed Cracks with Friction," *J. Mech. Phys. Solids*, **46** [1] 85–113 (1998).
- <sup>27</sup>B. R. Lawn, N. P. Padture, F. Guiberteau, and H. Cai, "A Model for Microcrack Initiation and Propagation Beneath Hertzian Contacts in Polycrystalline Ceramics," *Acta Metall.*, **42** [5] 1683–93 (1994). □